

# Spontaneous time-reversal symmetry breaking for spinless fermions on a triangular lattice

O. Tieleman,<sup>1</sup> O. Dutta,<sup>1</sup> M. Lewenstein,<sup>1,2</sup> and A. Eckardt<sup>1,3</sup>

<sup>1</sup>ICFO – Institut de Ciències Fotòniques, Parc Mediterrani de la Tecnologia, E-08860 Castelldefels, Spain

<sup>2</sup>ICREA – Institució Catalana de Recerca i Estudis Avançats, Lluís Companys 23, E-08010 Barcelona, Spain

<sup>3</sup>Max Planck Institute for the Physics of Complex Systems,  
Noethnitzer Str. 38, D-01187 Dresden, Germany.

(Dated: October 17, 2012)

As a minimal fermionic model with kinetic frustration, we study a system of spinless fermions in the lowest band of a triangular lattice with long-range repulsion. We find that the combination of interactions and kinetic frustration leads to spontaneous symmetry breaking in various ways. Time-reversal symmetry can be broken by two types of loop current patterns, a chiral one and one that breaks the translational lattice symmetry. Moreover, the translational symmetry can also be broken by a density wave forming a kagome pattern or by a Peierls-type trimerization characterized by enhanced correlations among the sites of certain triangular plaquettes (giving a plaquette-centered density wave). We map out the phase diagram as it results from leading order Ginzburg-Landau mean-field theory. Several experimental realizations of the type of system under study are possible with ultracold atoms in optical lattices.

Geometric frustration in classical and quantum many-body systems is a source of intriguing phenomena like extensive ground-state entropies, topological order, and exotic emergent low-energy physics [1–5]. It is naturally encountered in systems of antiferromagnetically coupled localized magnetic moments, arranged in a non-bipartite (e.g. triangular) lattice geometry that prohibits the favored antiparallel orientation between all pairs of neighboring moments. Recently, geometric frustration has also been induced to the *kinetics* of a system of ultracold bosonic atoms on a triangular lattice by dynamically inverting the sign of the tunneling matrix elements [6, 7]. For weak interaction the system shows spontaneous time-reversal (TR) symmetry breaking, whereas strong interactions are conjectured to lead to spin-liquid-like quantum disordered behaviour.

Here we investigate a minimal *fermionic* model with kinetic frustration: spinless fermions on a triangular lattice with off-site repulsion. It can be realized, e.g., with ultracold dipolar atoms or molecules in an optical lattice [8–10]. In this system kinetic frustration appears naturally as a consequence of fermi statistics. Namely, for filling well above one half the system is governed by the low-energy states of the fermionic holes whose kinetics is determined by the sign-inverted tunneling matrix elements. We focus on the weakly interacting regime and find that, depending on the filling, two types of loop currents can spontaneously emerge at experimentally accessible temperatures and break TR symmetry. One of them breaks the inversion symmetry of the lattice and is chiral, while the other one breaks the translational lattice symmetry. TR symmetry is broken neither as a consequence of coupling the kinetics to further degrees of freedom (such as spin or sublattice orbital freedom in the unit cell) nor in a process involving (quasi)long-range order in a continuous degree of freedom (i.e. bose condensation).

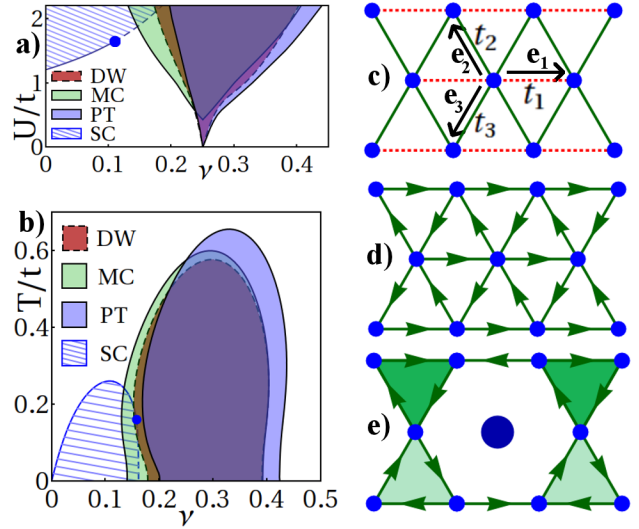


FIG. 1. (color online) a) and b) Phase diagram resulting from low-order Landau expansion of the mean-field free energy, with respect to interaction strength  $U/t$ , temperature  $T/t$ , and filling  $\nu$ . Solid (dashed) lines indicate second (first) order transitions;  $T/t = 0$  in a) and  $U/t = 2$  in b). c) Frustrated triangular lattice, with solid (dashed) lines representing negative (positive) hopping matrix elements. d) Pattern of staggered chiral plaquette currents (SC). e) Translational symmetry breaking by modulated currents (MC, arrows), a density-wave (DW) defining a kagome lattice (larger dot represents increased density), and Peierls-type trimerization [PT, triangular plaquettes with increased (lowered) correlations are indicated by dark (light) green shading].

Typically at least one of these two themes is encountered when TR symmetry is broken in fermionic systems; examples range from ferromagnetic metals to Mott-insulators with spin or orbital order, but comprise also exotic states

like chiral spin liquids (not featuring bose condensation) [11] or  $p + ip$  superconductors (not requiring spin) [12–15]. We also observe that the approximate nesting property of the fermi surface near hole filling of  $1/4$  gives rise to a rich spectrum of three different types of instabilities that break the translational symmetry: One of them leads to spatially modulated currents (MC) and has been mentioned already. The other two give rise to a density wave (DW) and to a Peierls-type trimerization (PT, a plaquette-centered density wave).

*Model* Our system is governed by the Hamiltonian

$$H = \sum_{\mathbf{r}} \left[ - \sum_{\mathbf{r}'=\mathbf{r}\pm\mathbf{e}_i} t_i \hat{c}_{\mathbf{r}}^\dagger \hat{c}_{\mathbf{r}'} + \frac{1}{2} \sum_{\mathbf{r}'\neq\mathbf{r}} V(\mathbf{r}-\mathbf{r}') \hat{c}_{\mathbf{r}}^\dagger \hat{c}_{\mathbf{r}'} \hat{c}_{\mathbf{r}'}^\dagger \hat{c}_{\mathbf{r}} \right]. \quad (1)$$

Here  $\hat{c}_{\mathbf{r}}$  denotes the annihilation operator for a fermion at the lattice site located at  $\mathbf{r}$ , and the vectors  $\mathbf{e}_i$  connect neighboring sites (see Fig. 1c). Repulsive interactions  $V(\mathbf{r})$  between distant sites can be achieved in various ways, e.g. by using dipolar atoms or molecules that are polarized perpendicular to the lattice plane [9, 16–20] or as a superexchange process between neighboring sites in a mixed Mott insulator of fermions and bosons [21–24]. For simplicity, in the following we assume isotropic nearest-neighbor interactions of strength  $U = V(\pm\mathbf{e}_i) > 0$ . The tunneling matrix elements along the three lattice directions  $\mathbf{e}_i$  shall be given by  $t_1 = -t$  and  $t_2 = t_3 = t$  with  $t > 0$  (see Fig. 1c), giving a  $\pi$ -flux through each plaquette. This sign configuration corresponds simply to studying holes instead of particles (which makes a difference in the non-bipartite triangular lattice) in a momentum shifted reference frame [25]. Another option would be to control the tunneling parameters via lattice shaking [6, 7]. The system of  $N$  particles on  $M$  sites (with filling  $\nu = N/M$ ) is characterized, moreover, by the temperature  $T$ .

The tunneling coefficients are such that the kinetic energy cannot be minimized between all neighboring sites at the same time, since negative (positive)  $t_i$  favor a single particle state with a relative phase of  $\pi$  (0) between two sites; the system is kinetically frustrated [6]. As a consequence, the single-particle dispersion relation  $\varepsilon(\mathbf{k}) = \sum_i 2t_i \cos(\mathbf{e}_i \cdot \mathbf{k})$  possesses two minima (see Fig. 2a). It is possible, however, to maximize the kinetic energy on every pair of neighboring sites, so the system is sensitive to the frustration for low filling only.

The double-well structure of the dispersion relation supports various interaction-driven instabilities. One type of instability results from interaction favoring particles to be close by in (quasi)momentum: The potential energy between two fermions with sharp momenta  $\mathbf{p}$  and  $\mathbf{p}+\mathbf{q}$  reads  $V(\mathbf{0}) - V(\mathbf{q}) \equiv \tilde{V}(\mathbf{q})$ , where the Fourier transform of the interaction  $V(\mathbf{q}) = M^{-1} \sum_i U \cos(\mathbf{e}_i \cdot \mathbf{q})$  decays with  $|\mathbf{q}|$  (see Fig. 2b), and the relevant momentum-dependent second term (the exchange term) obtains a

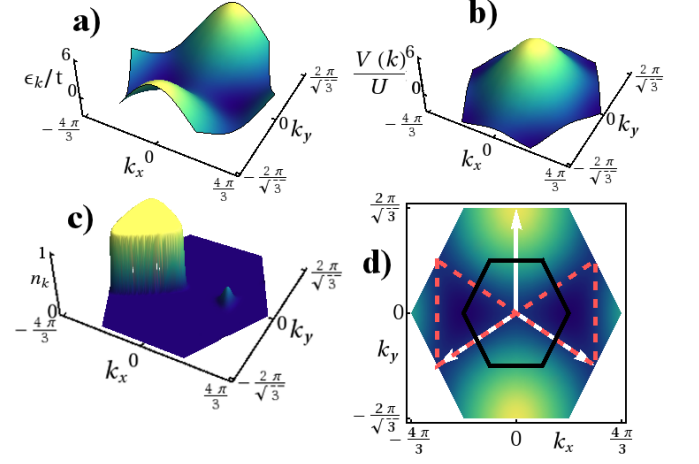


FIG. 2. (color online) a) Single particle spectrum with two minima as a consequence of frustration. b) Momentum representation of the nearest neighbor interaction of strength  $U$ . c) Momentum space density distribution for the staggered current phase (see Fig. 1d for the real-space signature). d) First Brillouin zone with nested Fermi surface (dashed ‘bowtie’-shaped line) and nesting vectors (white arrows); black line indicates reduced Brillouin zone.

minus sign from fermi statistics. For low filling this can, despite the kinetic energy cost, favor an imbalanced occupation of the two wells (see Fig. 2c) corresponding to staggered loop currents (SC) (see Fig. 1d).

Another source of instability appears near quarter filling  $\nu = 1/4$  where both minima are filled up completely, and the fermi surface is shaped like a bow-tie (Fig. 2d, dashed line) and becomes approximately nested. Namely,  $\varepsilon_{\mathbf{k}} - \varepsilon_{\mathbf{F}} \approx \varepsilon_{\mathbf{F}} - \varepsilon_{\mathbf{k}+\mathbf{Q}}$  with fermi energy  $\varepsilon_{\mathbf{F}}$  and the same nesting vector  $\mathbf{Q}$  for a significant fraction of momenta  $\mathbf{k}$  near the fermi surface, making the kinetic energy cost for spatial modulation described by  $\mathbf{Q}$  low [26]. The nesting occurs for the vectors  $\mathbf{Q}_j$  (Fig. 2d, white arrows) labeled  $j = 1, 2, 3$  such that  $\mathbf{e}_i \cdot \mathbf{Q}_j = (1 - \delta_{ij})\pi$  (since  $2\mathbf{Q}_j$  is a reciprocal lattice vector  $\mathbf{Q}_j$  and  $-\mathbf{Q}_j$  are equivalent). We find three different instabilities that break translational symmetry (see Fig. 1e) to be described below.

*Method* We use mean-field theory. In momentum representation,  $\hat{a}_{\mathbf{k}} = M^{-1/2} \sum_{\mathbf{r}} e^{-i\mathbf{k}\cdot\mathbf{r}} \hat{c}_{\mathbf{r}}$ , the interaction consists of terms  $V(\mathbf{q}) \hat{a}_{\mathbf{k}+\mathbf{q}}^\dagger \hat{a}_{\mathbf{p}-\mathbf{q}} \hat{a}_{\mathbf{p}} \hat{a}_{\mathbf{k}}$  that we approximate like  $\hat{a}_{\mathbf{k}}^\dagger \hat{a}_{\mathbf{l}}^\dagger \hat{a}_{\mathbf{p}} \hat{a}_{\mathbf{q}} \approx \xi_{\mathbf{kq}} \hat{a}_{\mathbf{l}}^\dagger \hat{a}_{\mathbf{p}} + \xi_{\mathbf{lp}} \hat{a}_{\mathbf{k}}^\dagger \hat{a}_{\mathbf{q}} - \xi_{\mathbf{kq}} \xi_{\mathbf{lp}} - \xi_{\mathbf{kp}} \hat{a}_{\mathbf{l}}^\dagger \hat{a}_{\mathbf{q}} - \xi_{\mathbf{lq}} \hat{a}_{\mathbf{k}}^\dagger \hat{a}_{\mathbf{p}} + \xi_{\mathbf{kp}} \xi_{\mathbf{lq}}$  while asking for self consistency  $\xi_{\mathbf{kp}} = \langle \hat{a}_{\mathbf{k}}^\dagger \hat{a}_{\mathbf{p}} \rangle$ . Allowing for spatial modulations described by the nesting vectors, we retain averages of the form  $\langle \hat{a}_{\mathbf{k}-\mathbf{Q}_j}^\dagger \hat{a}_{\mathbf{k}} \rangle$  with  $j = 0, 1, 2, 3$  where  $\mathbf{Q}_0 \equiv \mathbf{0}$ . Accordingly, we find single-particle correlations

$$\langle \hat{c}_{\mathbf{r}+\mathbf{e}_i}^\dagger \hat{c}_{\mathbf{r}} \rangle = \sum_{j=0}^3 e^{i\mathbf{r}\cdot\mathbf{Q}_j} c_{ij} \quad (2)$$

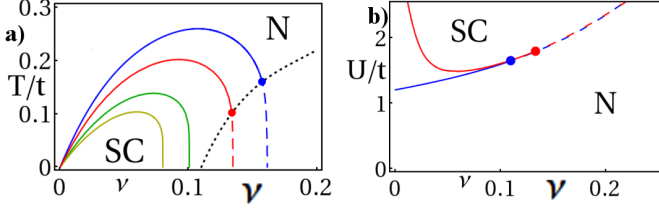


FIG. 3. (color online) Phase boundary of parameter region where staggered currents are expected (from low-order Landau expansion of the mean-field free energy) Solid (dashed) lines indicate second (first) order transitions. a)  $U/t = 1.5, 1.6, 1.8, 2$ , from small to large regions. b)  $T/t = 0$  (blue, crossing  $y$ -axis) and  $T/t = 0.2$  (red, not crossing  $y$ -axis).

where  $c_{ij} = M^{-1} \sum_{\mathbf{p}} e^{-i(\mathbf{p}-\mathbf{Q}_j) \cdot \mathbf{e}_i} \langle \hat{a}_{\mathbf{p}-\mathbf{Q}_j}^\dagger \hat{a}_{\mathbf{p}} \rangle$  (summing over one Brillouin zone). Defining  $\mathbf{e}_0 = \mathbf{0}$ , the local density  $n_{\mathbf{r}} = \langle \hat{c}_{\mathbf{r}}^\dagger \hat{c}_{\mathbf{r}} \rangle$  is related to the four averages  $c_{0j} \equiv \rho_j$ . The current from  $\mathbf{r}$  to  $\mathbf{r} + \mathbf{e}_i$ , namely  $J_i(\mathbf{r}) = 2t_i \text{Im} \langle \hat{c}_{\mathbf{r}+\mathbf{e}_i}^\dagger \hat{c}_{\mathbf{r}} \rangle / \hbar$ , is described by  $\text{Im} c_{i \neq 0j} \equiv I_{ij}$  (using the equivalence of  $\mathbf{Q}_j$  and  $-\mathbf{Q}_j$ ). We also define  $\text{Re} c_{i \neq 0j} \equiv R_{ij}$  for the real (non-current-generating) part of the correlations  $\langle \hat{c}_{\mathbf{r}+\mathbf{e}_i}^\dagger \hat{c}_{\mathbf{r}} \rangle$ . The terms  $\rho_0 = N/M$  and  $R_{i0}$  are non-zero already without symmetry breaking.

*Staggered currents* Well below quarter filling, nesting is irrelevant and only terms with  $j = 0$  are important. The free energy reads

$$F = -T \sum_{\mathbf{k}} \ln(1 + e^{-\omega_{\mathbf{k}}/T}) - \sum_{\mathbf{p}, \mathbf{q}} \tilde{V}(\mathbf{p} - \mathbf{q}) n_{\mathbf{p}} n_{\mathbf{q}},$$

with  $n_{\mathbf{k}} \equiv \langle \hat{a}_{\mathbf{k}}^\dagger \hat{a}_{\mathbf{k}} \rangle$  and dispersion relation  $\omega_{\mathbf{k}} = 2 \sum_{i=1}^3 [(t_i + U R_{i0}) \cos(\mathbf{k} \cdot \mathbf{e}_i) + U I_{i0} \sin(\mathbf{k} \cdot \mathbf{e}_i)]$ . If  $F$  is minimal for finite momentum imbalances  $I_{i0} = M^{-1} \sum_{\mathbf{p}} \sin(\mathbf{p} \cdot \mathbf{e}_i) n_{\mathbf{p}}$ , loop currents will emerge.

In order to learn when this happens, we apply perturbation theory within the imaginary time formalism and Landau expand the free energy in powers of the  $I_{i0}$ :

$$F \simeq F_0 + \mathbf{I}_1^T M \mathbf{I}_1 + \mathbf{I}_2^T K \mathbf{I}_2 + \mathcal{O}(I_{i0}^6) \quad (3)$$

where  $\mathbf{I}_n^T = (I_{10}^n, I_{20}^n, I_{30}^n)$  (with power  $n$  and transposition T) and where  $M$  and  $K$  are symmetric matrices. A second-order phase transition into a phase with finite averages  $\mathbf{I}_1^T = (-1, 1, 1)I$  occurs when  $m_2$ , the lowest eigenvalue of  $M$ , becomes negative, while higher-order contributions to  $F$  remain positive. The resulting phase boundaries are plotted as solid lines in Fig. 3. If the quartic term, with  $K_{ij} = \delta_{ij}|\eta| + (1 - \delta_{ij})\zeta$ , becomes negative for  $2\zeta < -|\eta|$  on the line defined by  $m_2 = 0$ , the phase transition becomes first-order (indicated by dashed lines in Fig. 3). Minimising  $F$  exactly at a few points in parameter space shows that the shift in the first-order phase boundary away from  $m_2 = 0$ , which enlarges the symmetry broken region, is very small (it is not taken into account in Fig. 3).

The current pattern that we find in the symmetry-broken phase at low densities is defined by  $J_i(\mathbf{r}) = -2t_i I_{i0} = J = \pm|J|$ , giving a staggered pattern of circular plaquette currents as shown in Fig. 1d. The state is two-fold degenerate and chiral in the sense that both TR and lattice inversion transform one solution into the other [11]. Experimentally this state can be identified by the momentum imbalance visible in time-of-flight absorption images.

The shape of the phase boundary (Fig. 3) can be understood as follows. For lower densities, the slope of the single-particle spectrum at the Fermi surface is flatter (see Fig. 2a), which explains why the critical interaction strength can be reduced when the filling is lowered. At high densities, moreover, the double-well structure of the dispersion relation (i.e. kinetic frustration) is not relevant anymore. If the filling is too low, however, a finite temperature  $T$  may overcome the energy scale  $U\nu$  of the interaction and destroy the currents altogether. Generally, increasing the temperature counteracts the clustering effect from momentum-space attraction, making a momentum space imbalance less favorable. We have performed exact diagonalizations for a small system (3 particles on 45 sites) at  $T = 0$ , and find an increased admixture of kinetic energy eigenstates with large  $|I_{i0}|$  for  $U/t \gtrsim 1$ , in support of the mean-field findings.

*Spatial modulation* Near quarter filling, where nesting becomes relevant, we have to take into account the additional possibility of spatial modulation, leading to a four-site unit cell. The mean-field Hamiltonian possesses four bands in a reduced Brillouin zone that has the same shape but only half the extent of the original one (Fig. 2d). Broken translational symmetry is indicated by finite averages  $\rho_j$ ,  $R_{ij}$ , or  $I_{ij}$  (with  $j \neq 0$ ) that open a gap between the lowest bands [27]. Expanding the free energy also with respect to those averages, in the leading (quadratic) order we find

$$F_{\text{mod}}^{(2)} = \sum_{j=1}^3 \left[ \mathbf{D}_j^T A \mathbf{D}_j + \mathbf{R}_j^T B \mathbf{R}_j + \mathbf{J}_j^T C \mathbf{J}_j + \lambda I_{jj}^2 \right] \quad (4)$$

with vectors  $\mathbf{D}_j^T = (\rho_j, R_{jj})$ ,  $\mathbf{R}_j^T = (R_{kj}, R_{lj})$  and  $\mathbf{J}_j^T = (I_{k,j}, I_{l,j})$  such that  $j \rightarrow k \rightarrow l$  under cyclic permutation, symmetric  $2 \times 2$  matrices  $A$ ,  $B$  and  $C$ , and coefficient  $\lambda > 0$ . The latter implies that  $I_{jj} = 0$  is favored. The remaining averages are coupled pairwise, with different nesting directions  $j$  uncoupled in quadratic order.

A DW instability is indicated when the lowest eigenvalue of  $A$  becomes negative. This defines the solid boundaries plotted in Fig. 4. In third order we find a term  $\Gamma \rho_1 \rho_2 \rho_3$  that couples the density modulations along the three directions  $j$ . It favors the four-fold degenerate kagome pattern shown in Fig. 1e with reduced correlations among the low-density sites due to the coupling to  $R_{jj}$ . The pattern with high and low occupations interchanged is disfavored (an obvious consequence

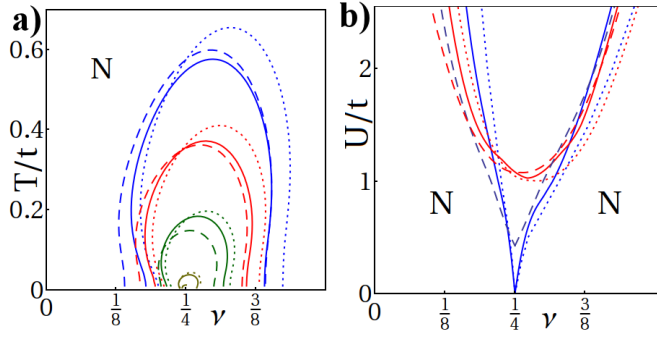


FIG. 4. (color online) Different types of instabilities that break the translational lattice symmetry are found inside the plotted boundaries. Solid, dotted, and dashed lines stand for instabilities leading to density-wave order, Peierls-type trimerization (i.e. plaquette-centered density-wave order), and a pattern of modulated currents, respectively. The transition to the density-wave order has to be first order. a)  $U/t = 0.5$  (inner curve), 1, 1.5, 2 (outer curves), b)  $T/t = 0$  (lower curves) and 0.1 (upper curves).

of nearest-neighbor repulsion on the triangular lattice). The third-order term also renders the transition first order and shifts the phase boundary slightly (not taken into account in Fig. 4). Exact diagonalization studies with 4 particles on 16 sites at  $T = 0$  reveal kagome DW patterns with a slight anisotropy (probably a finite size effect).

If the lowest eigenvalue of  $B$  turns negative (Fig. 4, dotted lines), an instability towards a Peierls-type modulation of nearest-neighbor correlations is found: Choosing spontaneously an embedded kagome pattern, the correlations  $\langle \hat{c}_{\mathbf{r}}^\dagger \hat{c}_{\mathbf{r}'} \rangle$  on the  $\triangle$  ( $\nabla$ ) triangular plaquettes of that pattern are increased (lowered); or vice versa (see Fig. 1e). This eight-fold degenerate Peierls trimerization breaks the inversion symmetry of the lattice and corresponds to a plaquette-centered DW.

Finally, if  $C$  acquires a negative eigenvalue (Fig. 4, dashed lines) an instability towards the formation of MC is indicated. One finds the current carrying bonds define a kagome lattice with circular currents of equal orientation around both types of triangular plaquettes ( $\triangle$  and  $\nabla$ ) and of opposite orientation around the hexagonal plaquettes (such that the finite plaquette fluxes of the mean-field Hamiltonian vanish when averaged over the unit cell). The eight-fold degeneracy of this pattern results from spontaneous breaking of both translational and TR symmetry.

The structure of the stability boundaries shown in Fig. 4 explains itself in an intuitive way. According to the nesting condition, interaction-induced spontaneous translational symmetry breaking occurs for filling near  $1/4$ , in a finite interval of filling factors that grows with increasing interaction. An interesting effect is that for a given interaction strength  $U/t$  this interval has its max-

imum extent at a non-zero temperature. The growth of the symmetry broken parameter region when a small temperature is switched on, might be explained by the fact that smoothening the fermi edge increases the number of participating momentum pairs for which the nesting condition is approximately fulfilled. However, for larger temperatures the order is eventually destroyed.

As visible in Figure 4 there is a large region in parameter space, where according to second Landau order all three nesting-driven types of symmetry breaking are favorable. As long as the spontaneous kagome patterns for the three match, they can in principle co-exist; their structures do not mutually exclude each other. This suggests that (at least as long as the order parameters are small such that low-order Landau terms dominate) the system might take advantage of realizing two or even all three of them at the same time, leading to a degeneracy of up to sixteen. However, generally it will depend on the energetics described by higher-order Landau terms that contain the coupling between the different orders, whether mean-field theory predicts such co-existences. Shifting and/or merging of the phase boundaries due to higher-order terms can be expected. Beyond mean-field theory this question can be answered by an experiment with ultracold atoms.

All three translational symmetry breaking orders (DW, MC, and PT) open up a gap between the lowest two bands of the mean-field dispersion relation in the reduced Brillouin zone. However, the momentum-space structure of the coupling that induces the gap depends on the type of order. Thus the three orders can be distinguished by the momentum distribution as it can be measured by time-of-flight absorption imaging.

We summarize our findings in Fig. 1 with subfigure a) and b) showing the combined phase diagram. For sufficiently large interactions there is a small parameter region where both the SC and the MC overlap. We expect both types of order to repel each other and it appears likely that higher order terms will remove this overlap region and predict a direct transition between both phases.

We conclude that kinetic frustration can give rise to rich physics in fermionic lattice models already for weak interactions. As an example we have considered the minimal model of spinless fermions on a triangular lattice for which we predict the emergence of chiral or modulated loop currents as well as Peierls-type trimerisation and density-wave instabilities. Our findings can be probed experimentally with ultracold fermionic atoms at accessible temperatures. Such an experiment would complement the recent observation of time-reversal symmetry breaking as a consequence of kinetic frustration in a system of bosonic atoms [7].

## ACKNOWLEDGEMENTS

OT thanks Achilleas Lazarides for helpful discussions and acknowledges funding from the Netherlands Organization for Scientific Research (NWO). Furthermore, we acknowledge funding from AAIL-Hubbard, EU STREP NAMEQUAM, ERC AdG QUAGATUA, Humboldt Stiftung, Joachim Herz Stiftung, University of Hamburg and the foundation universidad.es.

- 
- [1] X.-G. Wen, *Quantum Field Theory of Many-Body Systems* (Oxford University Press, New York, 2004).
  - [2] C. Lhuillier, arXiv:cond-mat/0502464 (2005).
  - [3] F. Alet, A. M. Walczak, and M. P. A. Fisher, *Physica A* **369**, 122 (2006).
  - [4] R. Moessner and A. P. Ramirez, *Physics Today* **59-2**, 24 (2006).
  - [5] S. Sachdev, *Nucl. Phys.* **4**, 173 (2008).
  - [6] A. Eckardt, P. Hauke, P. Soltan-Panahi, C. Becker, K. Sengstock, and M. Lewenstein, *EPL* **89**, 10010 (2010).
  - [7] J. Struck, C. Ölschläger, R. L. Targat, P. Soltan-Panahi, A. Eckardt, M. Lewenstein, P. Windpassinger, and K. Sengstock, *Science* **333**, 996 (2011).
  - [8] M. Lewenstein, A. Sanpera, and V. Ahufinger, *Ultracold Atoms in Optical Lattices: Simulating quantum many-body systems* (Oxford University Press, Oxford, UK, 2012).
  - [9] T. Lahaye, C. Menotti, L. Santos, M. Lewenstein, and T. Pfau, *Rep. Prog. Phys.* **72**, 126401 (2009).
  - [10] I. Bloch, J. Dalibard, and W. Zwerger, *Rev. Mod. Phys.* **80**, 885 (2008).
  - [11] X. G. Wen, F. Wilczek, and A. Zee, *Phys. Rev. B* **39**, 11413 (1989).
  - [12] W. Kohn and J. M. Luttinger, *Phys. Rev. Lett.* **15**, 524 (1965).
  - [13] G. Volovik, *JETP Letters* **70**, 609 (1999), 10.1134/1.568223.
  - [14] N. Read and D. Green, *Phys. Rev. B* **61**, 10267 (2000).
  - [15] D. A. Ivanov, *Phys. Rev. Lett.* **86**, 268 (2001).
  - [16] A. Griesmayer, J. Werner, S. Hensler, J. Stuhler, and T. Pfau, *Phys. Rev. Lett.* **94**, 160401 (2005).
  - [17] C. Trefzger, C. Menotti, B. Capogrosso-Sansone, and M. Lewenstein, *J. Phys. B* **44**, 193001 (2011).
  - [18] M. Lu, N. Q. Burdick, and B. L. Lev, *Phys. Rev. Lett.* **108**, 215301 (2012).
  - [19] K. K. Ni, S. Ospelkaus, D. Wang, G. Quemener, B. Neyenhuis, M. H. G. de Miranda, J. L. Bohn, J. Ye, and D. S. Jin, *Nature* **464**, 13241328 (2010).
  - [20] C.-H. Wu, J. Park, P. Ahmadi, S. Will, and M. Zwierlein, *Phys. Rev. Lett.* **109**, 085301 (2012).
  - [21] A. B. Kuklov and B. V. Svistunov, *Phys. Rev. Lett.* **90**, 100401 (2003).
  - [22] M. Lewenstein, L. Santos, M. Baranov, and H. Fehrmann, *Phys. Rev. Lett.* **92**, 050401 (2004).
  - [23] A. Eckardt and M. Lewenstein, *Phys. Rev. A* **82**, 011606(R) (2010).
  - [24] S. Sugawa, K. Inaba, S. Taie, R. Yamazaki, M. Yamashita, and Y. Takahashi, *Nature Phys.* **7** (2011).
  - [25] Starting from the standard (zero flux) situation with all three  $t_i > 0$ , a particle-hole transformation  $\hat{c}_{\mathbf{r}} \rightarrow \hat{c}_{\mathbf{r}}^\dagger$ , implying  $\hat{n}_{\mathbf{r}} = \hat{c}_{\mathbf{r}}^\dagger \hat{c}_{\mathbf{r}} \rightarrow 1 - \hat{n}_{\mathbf{r}}$ , inverts all tunneling matrix elements,  $t_i \rightarrow -t_j$ , while it leaves the interaction term (up to a constant) unchanged. A subsequent unitary transformation  $\hat{c}_{\mathbf{r}} \rightarrow \exp(i\mathbf{q} \cdot \mathbf{r})\hat{c}_{\mathbf{r}}$ , describing a shift in quasimomentum by  $\mathbf{q} = (0, 2\pi/\sqrt{3})$ , inverts (back) only  $t_2$  and  $t_3$ .
  - [26] T. M. Rice and G. K. Scott, *Phys. Rev. Lett.* **35**, 120 (1975).
  - [27] The gap opens along the  $\nu = 1/4$ -Fermi surface, forming an exotic star-shaped structure in the reduced Brillouin zone.